

Texture classification based on image (natural and horizontal) visibility graph constructing methods

Cite as: Chaos **31**, 013128 (2021); <https://doi.org/10.1063/5.0036933>

Submitted: 09 November 2020 . Accepted: 24 December 2020 . Published Online: 13 January 2021

Laifan Pei, Zhaohui Li, and  Jie Liu



[View Online](#)



[Export Citation](#)



[CrossMark](#)

ARTICLES YOU MAY BE INTERESTED IN

[A generalized permutation entropy for noisy dynamics and random processes](#)

Chaos: An Interdisciplinary Journal of Nonlinear Science **31**, 013115 (2021); <https://doi.org/10.1063/5.0023419>

[Transfer learning of chaotic systems](#)

Chaos: An Interdisciplinary Journal of Nonlinear Science **31**, 011104 (2021); <https://doi.org/10.1063/5.0033870>

[Estimating entropy rate from censored symbolic time series: A test for time-irreversibility](#)

Chaos: An Interdisciplinary Journal of Nonlinear Science **31**, 013131 (2021); <https://doi.org/10.1063/5.0032515>



AIP Advances
Mathematical Physics Collection

[READ NOW](#)

Texture classification based on image (natural and horizontal) visibility graph constructing methods

Cite as: Chaos 31, 013128 (2021); doi: 10.1063/5.0036933

Submitted: 9 November 2020 · Accepted: 24 December 2020 ·

Published Online: 13 January 2021



View Online



Export Citation



CrossMark

Laifan Pei,¹ Zhaohui Li,¹ and Jie Liu^{2,a)}

AFFILIATIONS

¹School of Mathematics and Computer Science, Wuhan Textile University, Wuhan, Hubei 430070, China

²Research Center of Nonlinear Science, Wuhan Textile University, Wuhan, Hubei 430070, China

^{a)}Author to whom correspondence should be addressed: liujie@wtu.edu.cn.

URL: <http://nonlinear.wtu.edu.cn/info/1068/1034.htm>

ABSTRACT

Texture classification is widely used in image analysis and some other related fields. In this paper, we designed a texture classification algorithm, named by TCIVG (Texture Classification based on Image Visibility Graph), based on a newly proposed image visibility graph network constructing method by Lacasa *et al.* By using TCIVG on a Brodatz texture image database, the whole procedure is illustrated. First, each texture image in the image database was transformed to an associated image natural visibility graph network and an image horizontal visibility graph network. Then, the degree distribution measure [$P(k)$] was extracted as a key characteristic parameter to different classifiers. Numerical experiments show that for artificial texture images, a 100% classification accuracy can be obtained by means of a quadratic discriminant based on natural TCIVG. For natural texture images, 94.80% classification accuracy can be obtained by a linear SVM (Support Vector Machine) based on horizontal TCIVG. Our results are better than that reported in some existing literature studies based on the same image database.

Published under license by AIP Publishing. <https://doi.org/10.1063/5.0036933>

During the last few decades, a **visibility graph (VG)** method was first proposed for time series analysis by Lacasa *et al.*,⁶ and it was successfully used to bridge the gap between time series and complex networks. It can differ in different nonlinear time series under the viewpoint of complex network analysis. Very recently, it was proven via numerical investigation that it can also be used to bridge the gap between the image and complex network. One can analyze images under the viewpoint of complex networks with the visibility algorithm as well.

I. INTRODUCTION

Increasing interest in complex network research has been motivated by intrinsic features of different area and application backgrounds, such as the analysis of the relationship between the structure and function, methods deriving from real application areas (understanding medical images, classification of time series, and recurrence images) from almost every field of scientific research.^{1,2}

During the recent several decades, literature studies published in different fields verified that almost all real data can be described as networks. Particularly, maps for bridging the gap between time

series and complex networks had attracted much attention in many fields, e.g., mathematics, physics, statistics, financial time series prediction, medical time series [such as electrocardiogram (ECG) and electroencephalogram (EEG) signals] classification,^{3–5} to name just a few.

Among those scientific advances, the visibility graph algorithm⁶ might be one of the most impressive methods in this direction. In the pioneer work of Lacasa *et al.*, they constructed a simple strategy to map time series into an associated network and encoded the inherent dynamical information in the related topological structure.⁶ They also proposed a mathematical analysis and some extended version of VG; see Refs. 7–10 and references therein. Those works paved the way for a graph-theoretical time series analysis and built a bridge between nonlinear dynamics and network science.

In this brief paper, we will investigate the classification problem of texture images^{20–22} via a network analysis method based on aforementioned VG⁶ and its modified version HVG (horizontal visibility graph). This is a new attempt for machine learning on image classification, which is different from a traditional image processing strategy.^{24–26} It is a natural extension and application of image VG proposed by the same group who proposed the VG algorithm.²⁷

In fact, there are some literature studies that have been published in the research fields of texture image classification and boundary shape analysis based on complex network modeling methods; see Refs. 15–18, etc. In Costa group's early attempt in this direction, they tried to construct hierarchical complex networks via similarity calculation between each pair of pixels of an image. They considered each pixel as a node and defined whether there were an existing connection between two pixels under a pre-setting threshold.¹⁶ Then, in Ref. 17, Gonçalves considered each pixel of a gray face image as nodes and defined strength of linkage according to the difference between two pixels under certain distance threshold. The proposed rotation invariant method was successfully used for face recognition field. Similar to Wesley's modeling strategy, Backes *et al.* further constructed a pixel distance threshold network model in Ref. 15, in which they considered the strength of linkages not only via values between two pixels, but also the physical distance between two pixels. That method was used for a texture image classification problem based on a network descriptor construction. At the same period, Backes *et al.* modeled a boundary shape into typical small world networks in Ref. 15. Backes *et al.* calculated the related numerical characters of associated complex network for the shape boundary. They found those characters are robust to normal noise, satisfying scale and rotation invariant. It becomes a useful method for shape classification and was widely used by potential users during the last decade. The main idea is to try to construct proper associated complex networks after the shape boundary was identified successfully (they considered each point on the boundary as nodes and constructed linkage between nodes under certain distance threshold). Very recently, the influence of boundary extraction operators on boundary shape classification algorithms based on complex networks was investigated in Ref. 19.

The rest of the paper is arranged as follows: In Sec. II, we will briefly recall the original visibility graph algorithm and some modified versions. The newly proposed image VG will be introduced in Sec. III. A new procedure for classification of texture images will be given in Sec. IV. Experiments on a classical image database will be carried out in Sec. V. Finally, a brief conclusion will be addressed in Sec. VI. Future work to be done is also mentioned briefly.

II. RECALL OF AN ORIGINAL VISIBILITY GRAPH ALGORITHM AND SOME MODIFIED VERSIONS

A complex network is formally defined as a graph that shows non-trivial topological features. Networks are made up of N entities called nodes interconnected by a set of L links, and they are commonly represented by an adjacency matrix, which is defined as

$$A_{ij} = \begin{cases} 1 & \text{if } \{i, j\} \in L, \text{ with } i \neq j, \\ 0 & \text{otherwise,} \end{cases} \quad (1)$$

where $i, j = 1, 2, \dots, N$ and L is the edge set of links. Therefore, the entries A_{ij} take into account the presence of a link between each pair of nodes. In this work, we considered each connection to be undirected ($A_{ij} = A_{ji}$) and unweighted, resulting in a binary and symmetrical adjacency matrix.

Recent research on complex systems shows that almost every real measured data with a certain relationship can be described as network objects. In classical mathematics, statistics descriptors are

the only tool to investigate nonlinear time series. This situation was slightly changed as the pioneer series work of mapping time series onto networks.⁶

We will first recall the useful visibility graph and the horizontal visibility graph algorithm, which were widely used to map time series into complex networks in related scientific research.

A. Natural visibility graph

The natural visibility graph (NVG) allows the visibility line between i and j to take any slope, whereas the horizontal visibility graph (HVG) is restricted to horizontal lines, as shown in Fig. 1.

For the time series $x = f(t)$, let $S = \{x_1, \dots, x_N\}$ be an ordered sequence of N real-valued data. A so-called visibility graph (VG) is an undirected graph of N nodes, where each node $i \in [1, N]$ is labeled according to the time order of its corresponding datum x_i . Hence, x_1 is mapped into node $i = 1$, x_2 into node $i = 2$, and so on. Then, two nodes i and j (assume $i < j$ without loss of generality) are connected by an (undirected) link if and only if one can draw a straight line connecting x_i and x_j that does not intersect any intermediate datum x_k , $i < k < j$. Equivalently, it can be seen that i and j will become two connected nodes if the following convexity visibility criteria is fulfilled,

$$x_k < x_i + \frac{k-i}{j-i}(x_j - x_i), \quad \forall(i < k < j). \quad (2)$$

That is, the adjacency matrix (A_{ij}) describing the VG as undirected and unweighted network is

$$A_{ij}^{(VG)} = A_{ji}^{(VG)} = \prod_{k=i+1}^{j-1} \Theta\left(x_j + (x_i - x_j) \frac{t_j - t_k}{t_j - t_i} - x_k\right), \quad (3)$$

where $\Theta(\bullet)$ is called the Heaviside function.

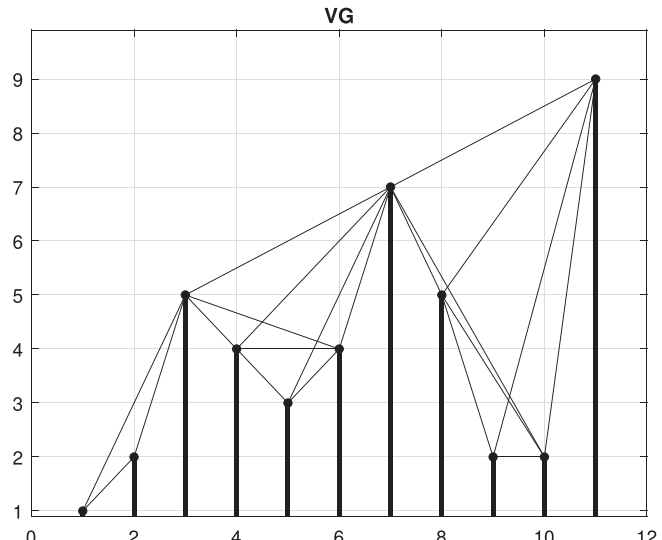


FIG. 1. Sample time series $([1, 2, 5, 4, 3, 4, 7, 5, 2, 2, 9])$ and its associated graph derived from the natural visibility graph algorithm.

B. Horizontal visibility graph

In a similar way, the so-called horizontal visibility graph (HVG) is defined as a subgraph of the VG, obtained by restricting the visibility criterion and imposing horizontal visibility instead. In this latter graph, two nodes i, j (assume $i < j$ without loss of generality) are connected by a link if and only if one can draw a horizontal line connecting x_i and x_j that does not intersect any intermediate datum x_k , $i < k < j$. Equivalently, i and j in the HVG are connected if the following ordering criterion is fulfilled:

$$x_k < \inf(x_i, x_j), \forall i < k < j. \quad (4)$$

There is an edge (i, j) if $x_k < \inf(x_i, x_j)$ for all k with $i < k < j$ so that

$$A_{ij}^{(HVG)} = A_{ji}^{(HVG)} = \prod_{k=i+1}^{j-1} \Theta(x_i - x_k) \Theta(x_j - x_k). \quad (5)$$

An aspect worth exploring is the relation between the data height and the node degree, that is, to study whether a functional relation between the height of a datum and the degree of its associated node holds. In this sense, define $P(k|x)$ as the conditional probability that a given node has degree k provided that it has height x ,

$$P(k|x) = \sum_{j=0}^{k-2} \frac{(-1)^{k-2}}{j!(k-2-j)!} [1 - F(x)]^2 \{In[1 - F(x)]\}^{k-2}. \quad (6)$$

Notice that probabilities are well normalized and that $\sum_{k=2}^{\infty} P(k|x) = 1$. Define an average value of the degree of a node associated with a datum of height x , $K(x)$, in the following way:

$$K(x) = \sum_{k=2}^{\infty} kP(k|x) = 2 - 2In[1 - F(x)]. \quad (7)$$

$F(x) \in [0, 1]$ and $In(x)$ are monotonically increasing functions. In addition, $K(x)$ is also monotonically increasing. The conclusion is that graph hubs (that is, the most connected nodes) are the data with the largest values, that is, the extreme events of the series. HVGs are outer-planar graphs with a Hamiltonian path. An illustration with the same time series in Fig. 1 was listed in Fig. 2.

C. Other modified visibility graphs

There are also some other versions of modified visibility graphs. For instance, Gao *et al.* proposed the limited penetrable visibility graph (LPVG) algorithm, which is verified to be robust to noise.^{11,12} Liu *et al.* proposed 2D and 3D time series visibility graphs, which can differ from periodical, regular, and chaotic time series.^{13,14} Since only VG and HVG were used in this paper, we will not address more on this topic. One can consult some newly published literature studies.

III. IMAGE VISIBILITY GRAPH ALGORITHM

In this section, the newly proposed image visibility graph will be introduced for further classification problems. In fact, one can easily extend the definition of VG and HVG to situations handling images according to the literature.²⁷

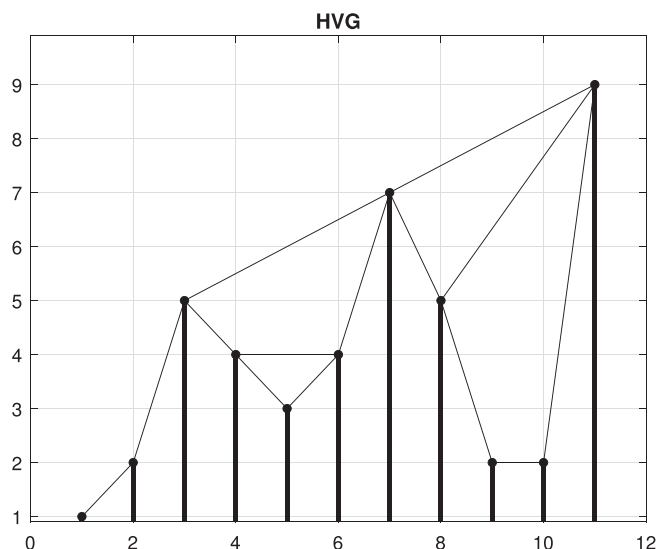


FIG. 2. Sample time series (same values as that in Fig. 11) and its associated graph derived from the horizontal visibility graph algorithm.

As we know, VG is constructed for ordered sequences along with time evolution. For images, it can be considered augmented one dimensional time series from two directions. One can build VG/HVG through these two directions. For simplicity, we just consider gray images here. One can consider constructing multiplex VG/HVG associated with the color image through three layers of a red-green-blue (RGB) image, i.e., consider red layer, green layer, and blue layer, respectively. Similar research can be designed and carried out based on other image models, such as the HSV (Hue, Saturation, Value) model.

A. INVG: Image natural visibility graph

The image visibility graph (IVG) is a graph of N^2 nodes, where each node is labeled by the indices of its corresponding datum I_{ij} such that two nodes ij and $i'j'$ are linked if

- $i = i'$ OR $j = j'$ OR $[i = j' \pm p \text{ AND } j = j' \pm p]$ for some integer p and
- I_{ij} and $I_{i'j'}$ are linked in the NVG definition algorithm, which is applied on the ordered sequence, which includes ij and $i'j'$.

Remark 1: Let I be a $N \times N$ matrix where $I_{ij} \in R$ and $N > 0$ (note at this point that n and N denote two different things). A toy model was proposed for understanding the basic algorithm of a image visibility graph shown in Fig. 3. The case of a 3×3 gray image is converted to the corresponding INVG for algorithm illustration in the cases of with or without lattice structures. It should be pointed out that in Ref. 27, one can easily see that the illustration figure is wrong in one direction. (We had corrected it here; see Fig. 3.) One can choose an algorithm without a lattice structure to reduce the number of links during creation of associated networks for a typical image database. It depends on the time consumption of the whole procedure. The illustration figure can be seen in Fig. 3.



Local IVG illustration.

(Left): Algorithm with lattice.

(Right): Algorithm without lattice.

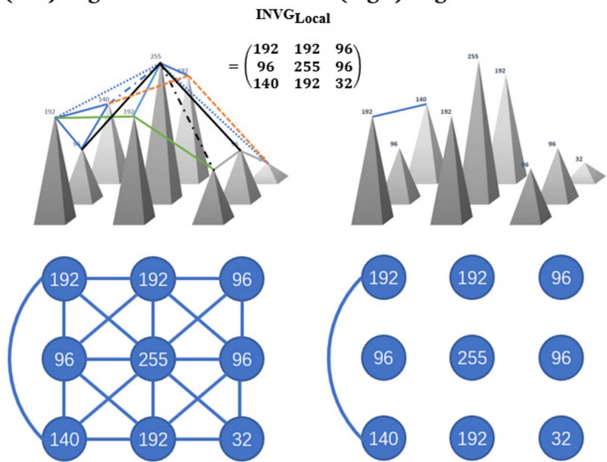


FIG. 3. Local illustration of an image visibility graph algorithm used on a typical picture (bottom left corner of Lena), where the node properties inherit the spatial local information of the pixels according to the IVG algorithm with and without the lattice structure. (It is a modified illustration figure similar but different from Ref. 27.)

We also gave the details of the algorithm in Fig. 4. Associated natural visibility graph networks of a typical texture image patch with and without a lattice structure are listed in Fig. 5.

Remark 2: In our numerical investigation procedure, both experiments on algorithms with and without lattice had been calculated, respectively. Similar results were obtained, and we will report the average best results here, where the INVG algorithm was without lattice and the image horizontal visibility graph (IHVG) algorithm was with lattice. It showed that both methods were effective.

B. IHVG: Image horizontal visibility graph

The image horizontal visibility graph (IHVG) follows equivalently if one uses IHVG instead of INVG in the second linkage

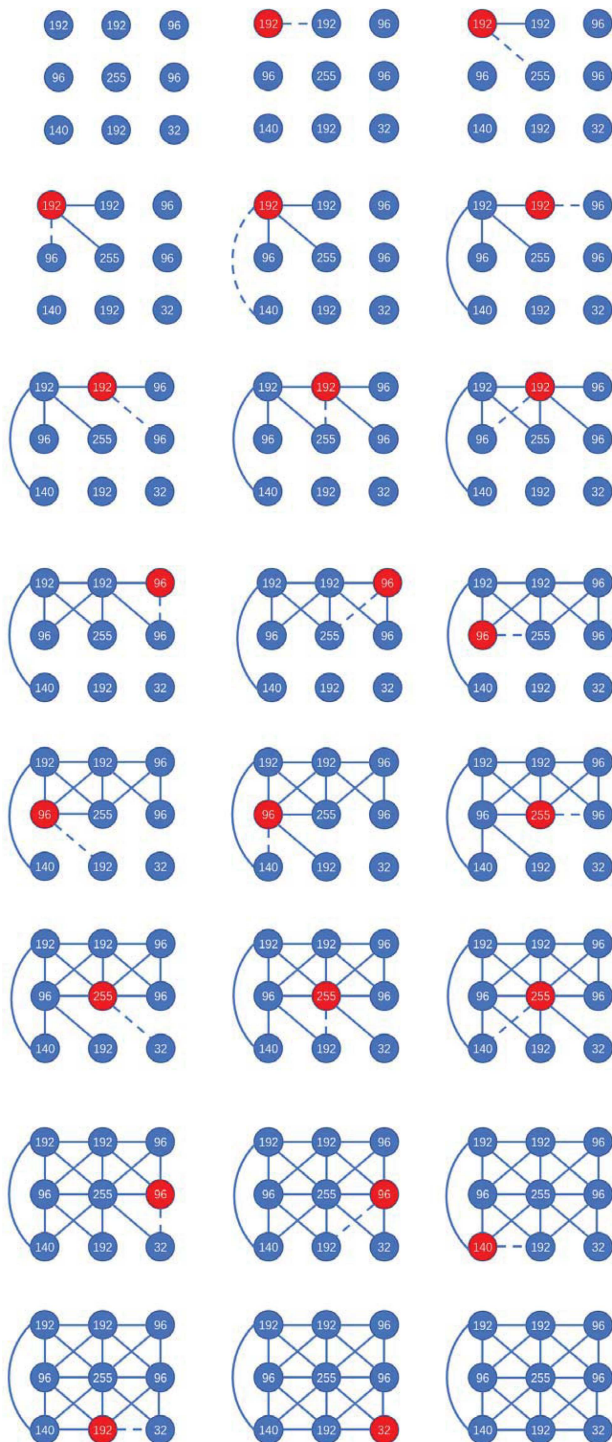


FIG. 4. Details of local illustration about an image visibility graph algorithm with a lattice structure shown in Fig. 3. (For the case of the situation without a lattice, one can just delete all neighbor links from all directions.)

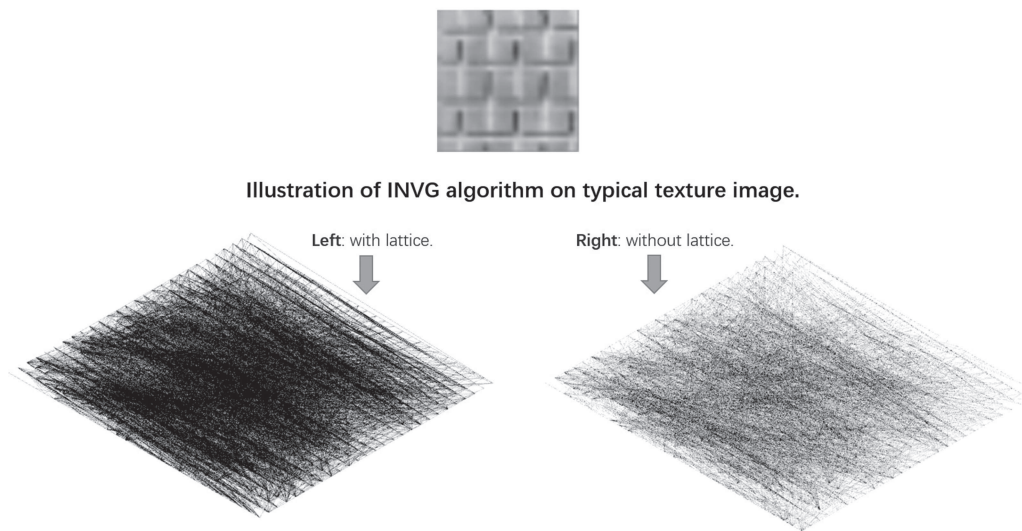


FIG. 5. Associated natural visibility graph networks of a typical texture image with and without a lattice structure.

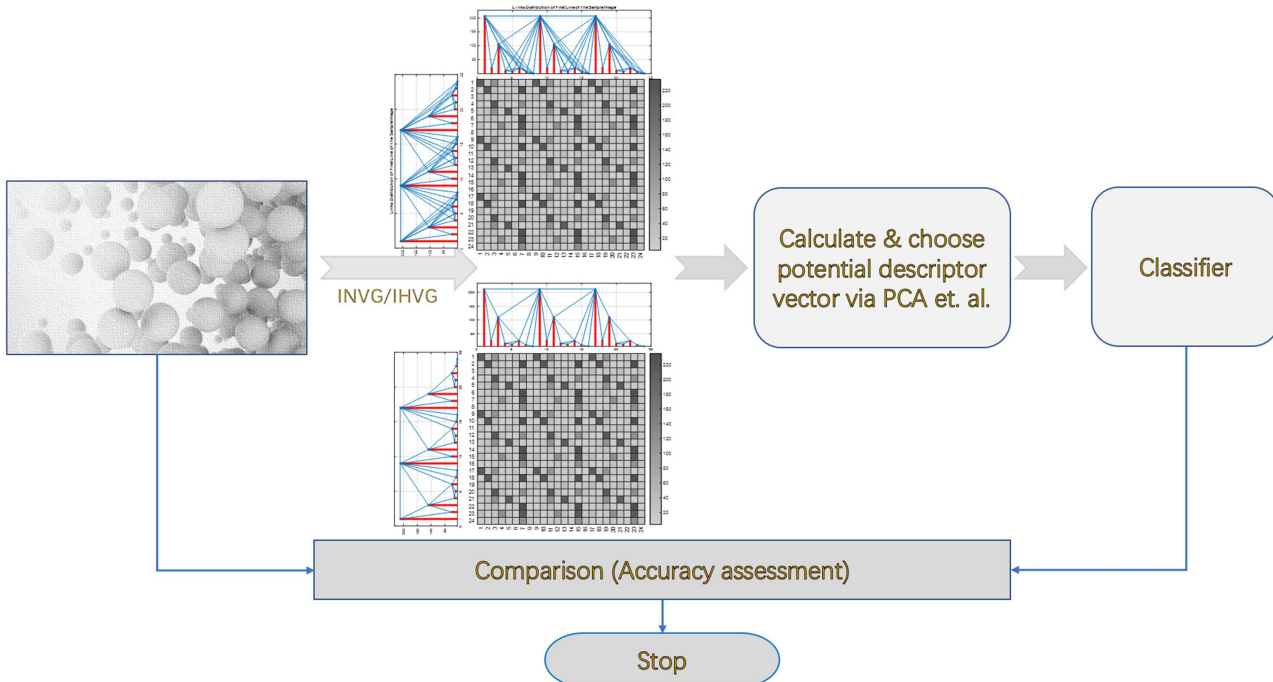


FIG. 6. The TCIVG algorithm's main procedure.

condition. Note that this definition coincides with the definition of an INVG/IHVG in the so-called FCC extension class, this being one of other possibilities for the analysis of high-dimensional scalar fields, which it is adopted here for convenience as this particular one is well-fitted for image processing.

The algorithm can also be simplified after some factors are taken into account, and it can lead to a visibility adjacency matrix with a general form as follows:

$$A = \begin{pmatrix} 0 & \cdots & a_{1,N} \\ a_{N,1} & \cdots & 0 \end{pmatrix}. \quad (8)$$

Nodes i and j are connected through an undirected edge ($a_{ij} = a_{ji} = 1$) from two directions according to classical NVG and HVG algorithms. The degree plot (also known as a k-filtered image) is derived from the spatial local information of pixels $\{x_1, \dots, x_N\}$.

An illustration of such an algorithm on a patch of a typical texture image is shown in Fig. 5 as well.

IV. TCIVG: FLOW CHART AND ALGORITHM ILLUSTRATION

Based on the IVG algorithm, we designed a procedure to fulfill classification of texture images under a certain background. The algorithm procedure can be described as that in Fig. 6.

The algorithm flow chart is listed as that in Fig. 7.

One can use that standard procedure to fulfill some classification tasks on gray image databases. We will show the effectiveness of such a procedure in Sec. V.

V. EXPERIMENTS AND DISCUSSIONS

In order to verify the effectiveness of a TCIVG algorithm, the famous Brodatz texture image database is selected for further numerical investigation.^{29,30} In a Brodatz texture image database, the first 12 images are natural texture images, which are indexed as D04, D05, D15, D19, D51, D68, D71, D72, D80, D87, D103, and D106. The last 12 are the artificial texture images, which are indexed as D01, D11, D20, D26, D46, D47, D48, D49, D95, D96, D101, and D102. According to our designed flow chart in Fig. 7, we will check the classification results based on these labels. Altogether, 24 kinds of texture images are selected and used as experimental texture images for classification (see Fig. 8).

In this paper, all numerical experiments were carried out on a personal computer with 2.9 GHz Intel Core i5 processor, 16 GB memory.

In the numerical experiment part, each chosen texture image was transformed onto the associated IVG or IHVG networks first, as described in the flow chart of Fig. 6. Their degree distribution $P(k)$ was extracted as explanatory variables, which were given as input vectors of a different classifier. The classification results are listed as those in Tables I, II and III of each subsection, respectively.

A. Classification of the whole texture image set

All of the whole 24 kinds of 640×640 pixel texture images selected in this experiment were divided into 160×160 pixel images

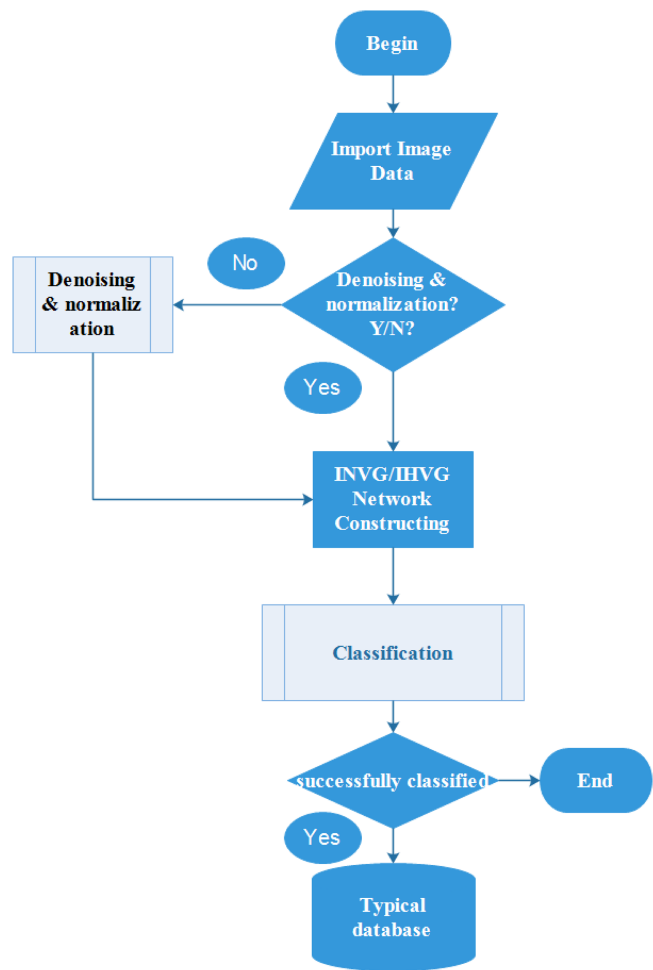


FIG. 7. The TCIVG algorithm flow chart.

by 4×4 non-overlapping to form the experimental database (see Fig. 8).

Each texture image of a Brodatz texture image database is transformed into the corresponding IVG and IHVG. Its degree distribution $P(k)$ is extracted and then given as input to a different classifier (see Table I). The related bar chart is also proposed in Fig. 9.

Experiments demonstrate the feasibility of our approach with short system responding time and high accuracy that is 91.4%.

B. Classification of natural texture images

12 kinds of 640×640 pixel natural texture images selected in this experiment are divided into 160×160 pixel images by 4×4 non-overlapping to form the experimental database (see Fig. 10).

Each natural texture image is transformed into the corresponding IVG and IHVG. Its degree distribution $P(k)$ is extracted and then

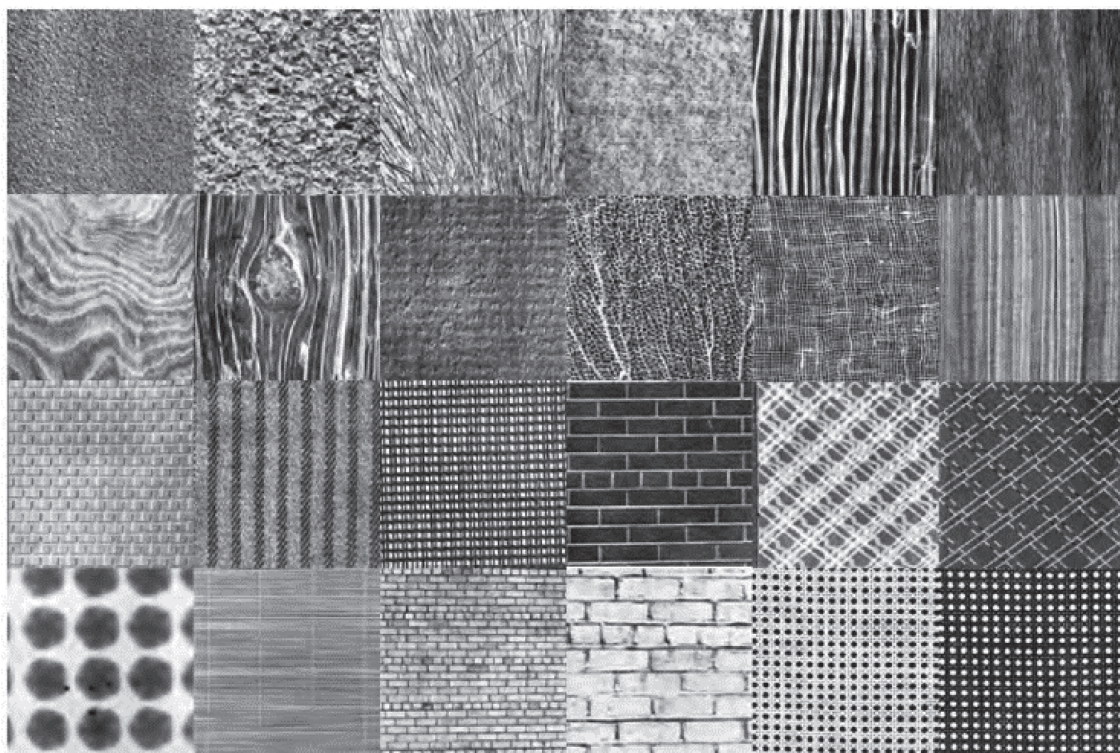


FIG. 8. 24 typical experimental texture images from the Brodatz texture image database.

TABLE I. Classification results on the whole Brodatz texture image database, where average best results are listed here, where the INVG algorithm is without lattice and the IHVG algorithm is with lattice.

| Classifier | Test accuracy INVG (%) | Test accuracy IHVG (%) | Test time INVG (s) | Test Time IHVG (s) |
|------------------------------|------------------------|------------------------|--------------------|--------------------|
| Fine tree | 82.3 | 75.0 | 7.3464 | 0.8547 |
| Medium tree | 64.6 | 75.0 | 6.7230 | 1.3859 |
| Linear discriminant | 84.1 | 86.7 | 6.0464 | 1.6277 |
| Quadratic discriminant | 91.4 | 87.8 | 7.2321 | 2.5177 |
| Gaussian naïve Bayes | 89.1 | 86.7 | 7.7876 | 2.9871 |
| Kernel naïve Bayes | 87.2 | 86.7 | 12.771 | 5.9500 |
| Linear SVM | 84.1 | 87.0 | 36.980 | 17.018 |
| Quadratic SVM | 89.3 | 90.1 | 38.795 | 18.484 |
| Cubic SVM | 89.8 | 88.5 | 39.273 | 18.932 |
| Fine Gaussian SVM | 88.8 | 88.0 | 42.220 | 20.878 |
| Medium Gaussian SVM | 71.1 | 75.3 | 54.191 | 32.774 |
| Fine KNN (k-NearestNeighbor) | 88.3 | 88.5 | 40.019 | 19.168 |
| Medium KNN | 84.9 | 86.7 | 40.366 | 19.626 |
| Cosine KNN | 81.5 | 72.4 | 42.304 | 20.768 |
| Cubic KNN | 85.7 | 86.5 | 43.320 | 20.689 |
| Weighted KNN | 89.1 | 89.8 | 43.237s | 21.125 |
| Boosted trees | 79.9 | 79.4 | 47.559 | 23.606 |
| Bagged tree | 85.7 | 83.1 | 47.428 | 24.076 |
| Subspace discriminant | 84.6 | 86.2 | 50.697 | 26.247 |
| Subspace KNN | 88.0 | 83.1 | 50.508 | 26.691 |
| RUSBoosted trees | 72.9 | 71.4 | 53.472 | 29.161 |

TABLE II. Classification results on natural texture images from a Brodatz texture image database, where average best results are listed here, where the INVG algorithm is without lattice and the IHVG algorithm is with lattice.

| Classifier | Test accuracy INVG (%) | Test accuracy IHVG (%) | Test time INVG (s) | Test time IHVG (s) |
|------------------------|------------------------|------------------------|--------------------|--------------------|
| Fine tree | 85.9 | 84.9 | 0.9981 | 5.6889 |
| Medium tree | 85.9 | 84.9 | 5.5212 | 5.4003 |
| Linear discriminant | 85.9 | 93.2 | 5.3319 | 5.2505 |
| Quadratic discriminant | 87.5 | 91.7 | 5.4443 | 5.1176 |
| Gaussian naïve Bayes | 84.9 | 91.1 | 4.8658 | 5.0685 |
| Kernel naïve Bayes | 84.4 | 88.5 | 3.0301 | 7.8815 |
| Linear SVM | 85.9 | 94.8 | 10.424 | 11.175 |
| Quadratic SVM | 85.9 | 93.2 | 10.788 | 11.071 |
| Cubic SVM | 81.3 | 90.6 | 11.286 | 10.976 |
| Fine Gaussian SVM | 87.0 | 92.7 | 11.207 | 10.896 |
| Medium Gaussian SVM | 73.4 | 79.2 | 10.606 | 10.817 |
| Fine KNN | 86.5 | 89.6 | 9.842 | 11.845 |
| Medium KNN | 84.4 | 90.1 | 10.426 | 11.781 |
| Cosine KNN | 77.6 | 87.5 | 11.373 | 11.635 |
| Cubic KNN | 83.3 | 89.1 | 11.307 | 11.272 |
| Weighted KNN | 87.0 | 91.1 | 10.795 | 11.686 |
| Bagged tree | 84.9 | 84.8 | 13.953 | 14.131 |
| Subspace discriminant | 85.9 | 93.2 | 13.856 | 14.639 |
| Subspace KNN | 82.3 | 89.6 | 13.793 | 14.577 |

given in input to a different classifier (see Table II). The related bar chart is also proposed in Fig. 11.

The experimental results show that the classifier has higher classification precision that is 94.8% and is more efficient than other classifiers.

C. Classification of artificial texture images

12 kinds of 640×640 pixel artificial texture images selected in this experiment are divided into 160×160 pixel images by 4×4 non-overlapping to form the experimental database (see Fig. 12).

TABLE III. Classification results on artificial texture images from a Brodatz texture image database, where average best results are listed here, where the INVG algorithm is without lattice and the IHVG algorithm is with lattice.

| Classifier | Test accuracy INVG (%) | Test accuracy IHVG (%) | Test time INVG (s) | Test time IHVG (s) |
|------------------------|------------------------|------------------------|--------------------|--------------------|
| Fine tree | 94.8 | 87.0 | 5.5687 | 6.2842 |
| Medium tree | 94.8 | 87.0 | 5.4320 | 5.7148 |
| Linear discriminant | 96.4 | 94.3 | 5.2545 | 6.7643 |
| Quadratic discriminant | 100 | 93.8 | 5.1541 | 6.6561 |
| Gaussian naïve Bayes | 98.4 | 95.3 | 5.0684 | 6.2062 |
| Kernel naïve Bayes | 97.9 | 96.4 | 7.9537 | 7.8606 |
| Linear SVM | 97.9 | 92.2 | 11.152 | 12.367 |
| Quadratic SVM | 98.4 | 93.8 | 11.402 | 12.651 |
| Cubic SVM | 98.4 | 92.7 | 11.010 | 12.563 |
| Fine Gaussian SVM | 99.0 | 94.8 | 10.914 | 12.481 |
| Medium Gaussian SVM | 94.8 | 80.7 | 10.810 | 12.396 |
| Fine KNN | 99.5 | 94.3 | 11.727 | 12.336 |
| Medium KNN | 97.4 | 94.8 | 12.296 | 12.772 |
| Cosine KNN | 94.8 | 83.3 | 12.197 | 12.62 |
| Cubic KNN | 97.9 | 95.3 | 11.780 | 13.017 |
| Weighted KNN | 98.4 | 95.8 | 11.717 | 12.482 |
| Bagged tree | 93.2 | 86.5 | 14.098 | 15.588 |
| Subspace discriminant | 96.9 | 94.3 | 14.615 | 15.492 |
| Subspace KNN | 99.0 | 89.1 | 14.541 | 15.862 |

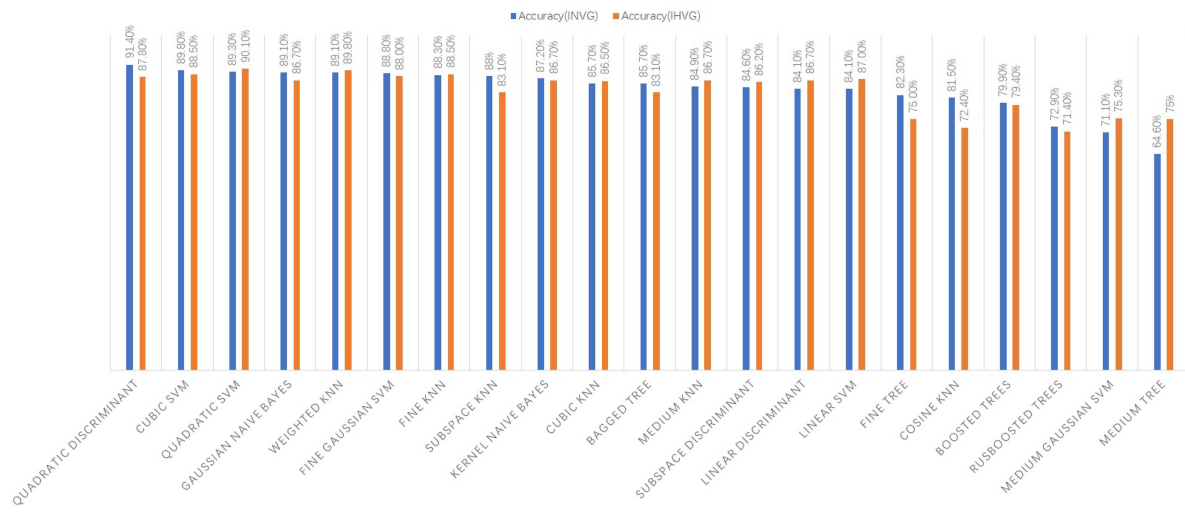


FIG. 9. Numerical results with the whole texture images of Brodatz texture image data sets. One can see that 91.4% accuracy was obtained via a quadratic discriminant classifier via INVG.

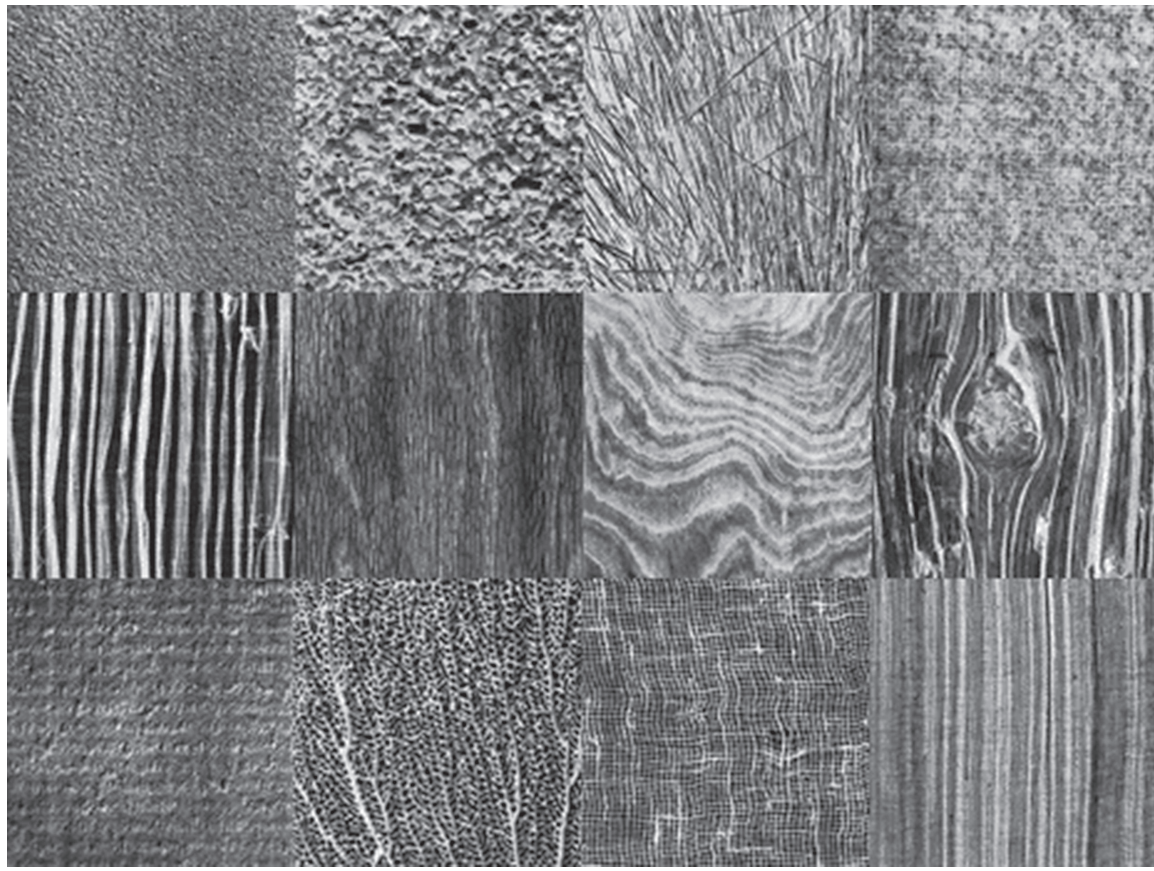


FIG. 10. The selected 12 kinds of 640 × 640 pixel natural texture images are from Brodatz texture image data sets.

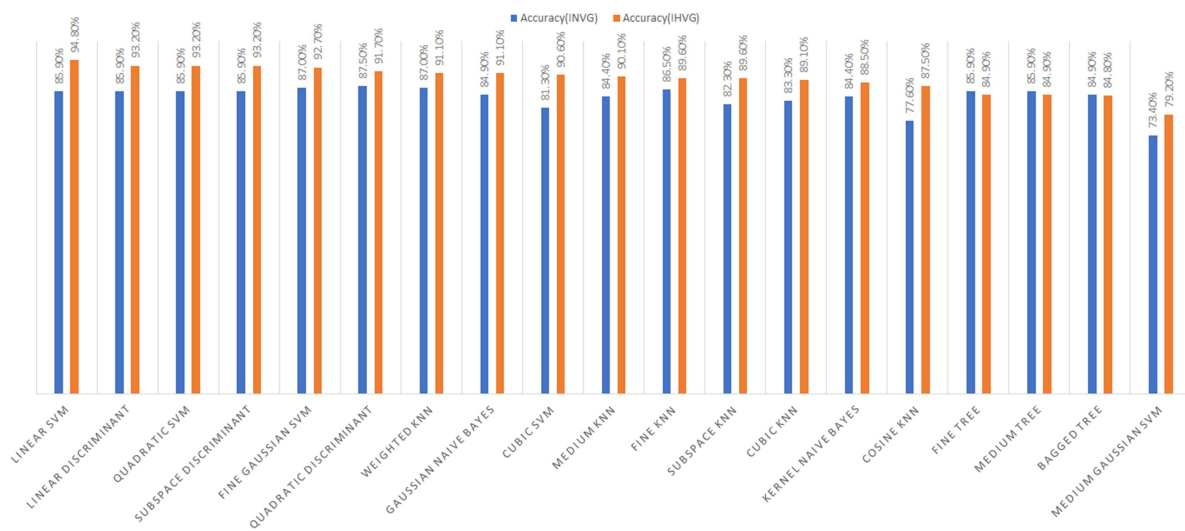


FIG. 11. Numerical results with selected 12 kinds of 640×640 pixels, which are natural texture images from Brodatz texture image data sets. One can see that 94.8% accuracy was obtained via a linear SVM classifier via IHVG.

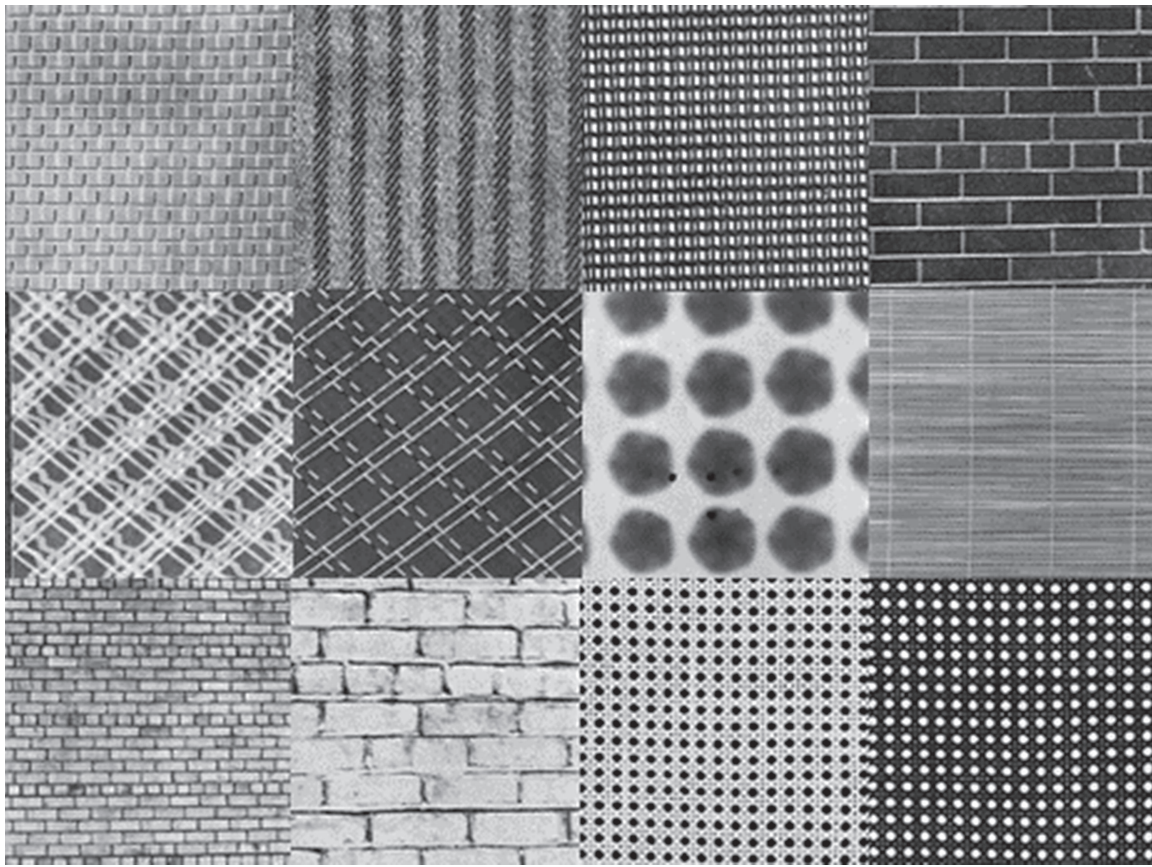


FIG. 12. The selected 12 kinds of 640×640 pixel artificial texture images are from Brodatz texture image data sets.

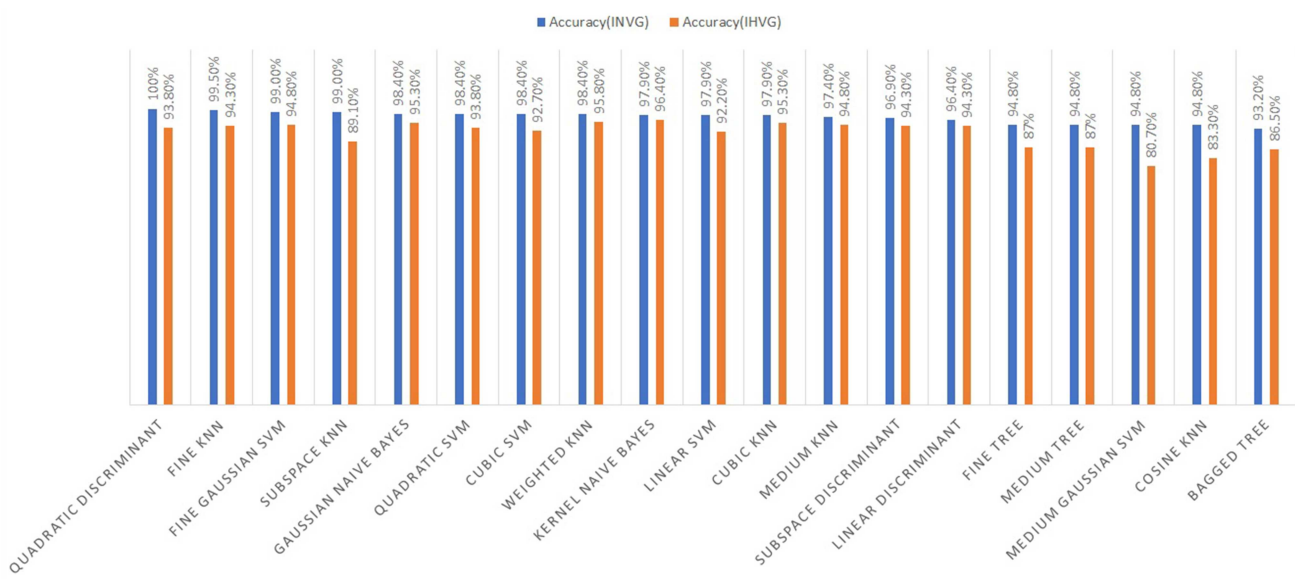


FIG. 13. Numerical results with selected 12 kinds of 640 × 640 pixels, which are artificial texture images from Brodatz texture image data sets. One can see that 100% accuracy was obtained via a quadratic discriminant classifier via IVNG.

Each artificial texture image is transformed into the corresponding IVG and IHVG. Its degree distribution $P(k)$ is extracted and then given in input to a different classifier (Table III). The related bar chart is also proposed in Fig. 13.

D. Comparison with some existing literature studies

In this section, we will give some comparison results for reference.

The classification methods mentioned here include the Angular Radial Transform (ART) method, the Gray-level Co-occurrence Matrix (GLCM) method, the Similar Distance Measuring (SDM) method, and the Belief Rule Base (BRB) method. In Ref. 22, the

ART method was used for the same image database used in our paper. One can easily found that the IVNG approach increased the accuracy of texture categorization than existing literature studies, such as the result via the Angular Radial Transform (ART) method whose accuracy is only 90.625% even just for an artificial database. In Ref. 23, the Gray-level Co-occurrence Matrix (GLCM) method, the Similar Distance Measuring (SDM) method, and the Belief Rule Base (BRB) method are tested on the same image database. One can also see that the accuracy was obviously improved via the IVNG/IHVG method used here as well.

We also compared with the existing results using a complex network modeling method reported in Ref. 18. For the Brodatz texture image database, the best result based on the energy feature

TABLE IV. Comparison results with some existing literature studies.

| Classifier | Test accuracy of natural images (%) | Test accuracy of artificial images (%) | Test accuracy of all hybrid images (%) |
|-------------------------------------------|-------------------------------------|----------------------------------------|-------------------------------------------------------------------------------------------------------------------|
| TCIVG (our result) | 94.8000 | 100.000 | 91.4000 |
| ART ²² | 79.1667 | 90.6250 | N/A |
| GLCM+SDM ²³ | 76.0416 | 89.5833 | N/A |
| GLCM+BRB ²³ | 80.2083 | 92.7083 | N/A |
| ART+SDM ²³ | 79.1667 | 90.6250 | N/A |
| ART+BRB ²³ | 83.3333 | 96.8750 | N/A |
| Backes's CN ¹⁸ | N/A | N/A | 89.8600 (Best results based on energy feature complex network modeling method with 36 descriptors) |
| Backes's combination method ¹⁸ | N/A | N/A | 95.2700 (best results based on different histogram features and their combination method with 108 descriptors) |

complex network modeling method with 36 descriptors is 89.8600%, which is lower than our best results. The best result based on different histogram features and their combination method with 108 descriptors is 95.2700%, which is better than our best result of 91.4000%. However, it should be pointed out that the difficulty of calculation of 108 descriptors and the degree distribution is not the same. Therefore, in real applications, one can choose a balance between test accuracy and calculation complexity. The classification methods based on INVG and IHVG algorithms might be useful as well. In **Table IV**, all calculation results were listed for further reference.

Overall, our numerical results showed that for both natural texture images and artificial texture images, the performance of the TCIVG algorithm in texture feature extraction can have satisfactory performance. One can easily extend the TCIVG algorithm for similar application situation according to our procedure. Such a procedure can even be used for classification of color images since IVG is also extendable for RGB color images according to the description mentioned in Refs. 27 and 28. We will give some attempt to fulfill such tasks in the near future.

VI. CONCLUSION AND OUTLOOK

As a fast developing tool for transforming time series into complex networks, Visibility Graph (VG) and its modified versions had been widely used on time series. Very recently, it was also successfully extended to image processing fields. In this paper, we also tried to extend it to the field of classification of texture images. We designed a texture classification algorithm, named TCIVG, based on L. Lacasa's image visibility graph constructing method. Classification of Brodatz texture image database procedures are illustrated by using TCIVG. Numerical experiments verified that our numerical results are better than some existing literatures on the same image database.

In the near future, we will try to extend 2D TCIVG to 3D TCIVG, which might be useful for a 3D medical image in an intelligent medical image diagnosis. A potential micro-structure might be detected via 3D TCIVG, which can play the critical role of complex 3D scenes. Therefore, creating scientific 3D TCIVG algorithms might also be useful for image classification and image processing. Also, we will try to design some related algorithms that are robust to noise.

ACKNOWLEDGMENTS

This work was supported by the National Natural Science Foundation of China (NNSFC) under Grant No. 61573011.

DATA AVAILABILITY

The data that support the findings of this study are available from the corresponding author upon reasonable request.

REFERENCES

- ¹Y. Tang, J. Kurths, W. Lin, E. Ott, and L. Kocarev, "Introduction to Focus Issue: When machine learning meets complex systems: Networks, chaos, and nonlinear dynamics," *Chaos* **30**(6), 063151 (2020).
- ²C. H. Comin, T. Peron, F. N. Silva, D. R. Amancio, F. A. Rodrigues, and L. D. F. Costa, "Complex systems: Features, similarity and connectivity," *Phys. Rep.* **861**, 1–41 (2020).
- ³M. Ahmadlou, H. Adeli, and A. Adeli, "Improved visibility graph fractality with application for the diagnosis of autism spectrum disorder," *Physica A* **391**(20), 4720–4726 (2012).
- ⁴S. Jiang, C. Bian, X. Ning, and Q. D. Ma, "Visibility graph analysis on heartbeat dynamics of meditation training," *Appl. Phys. Lett.* **102**(25), 253702 (2013).
- ⁵S. Sannino, S. Stramaglia, L. Lacasa, and D. Marinazzo, "Visibility graphs for fMRI data: Multiplex temporal graphs and their modulations across resting-state networks," *Netw. Neurosci.* **1**(3), 208–221 (2017).
- ⁶L. Lacasa, B. Luque, F. Ballesteros, J. Luque, and J. C. Nuno, "From time series to complex networks: The visibility graph," *Proc. Natl. Acad. Sci. U.S.A.* **105**(13), 4972–4975 (2008).
- ⁷B. Luque, L. Lacasa, F. Ballesteros, and J. Luque, "Horizontal visibility graphs: Exact results for random time series," *Phys. Rev. E* **80**(4), 046103 (2009).
- ⁸A. M. Nuez, L. Lacasa, J. P. Gomez, and B. Luque, "Visibility algorithms: A short review," *New Front. Graph Theory* **6**, 119–152 (2012).
- ⁹L. Lacasa, "On the degree distribution of horizontal visibility graphs associated with Markov processes and dynamical systems: Diagrammatic and variational approaches," *Nonlinearity* **27**(9), 2063 (2014).
- ¹⁰J. F. Donges, R. V. Donner, and J. Kurths, "Testing time series irreversibility using complex network methods," *Europhys. Lett.* **102**(1), 10004 (2013).
- ¹¹Z. K. Gao, M. Small, and J. Kurths, "Complex network analysis of time series," *Europhys. Lett.* **116**(5), 50001 (2017).
- ¹²T. T. Zhou, N. D. Jin, Z. K. Gao, and Y. B. Luo, "Limited penetrable visibility graph for establishing complex network from time series," *Acta Phys. Sin.* **61**(3), 030506 (2012).
- ¹³J. Liu and Q. Li, "Planar visibility graph network algorithm for two dimensional time series," in *2017 29th Chinese Control And Decision Conference (CCDC)* (IEEE, 2017), pp. 1352–1357.
- ¹⁴J. Liu, H. Liu, Z. Huang, and Q. Tang, "Differ multivariate timeseries from each other based on a simple multiplex visibility graphs technique," in *2015 Sixth International Conference on Intelligent Control and Information Processing (ICICIP)* (IEEE, 2015), pp. 289–295.
- ¹⁵A. R. Backes, D. Casanova, and O. M. Bruno, "A complex network-based approach for boundary shape analysis," *Pattern Recognit.* **42**(1), 54–67 (2009).
- ¹⁶L. da F. Costa, P. V. Boas, F. Silva, and F. Rodrigues, "A pattern recognition approach to complex networks," *J. Stat. Mech.: Theory Exp.* **2010**(11), P11015.
- ¹⁷W. N. Gonçalves, J. De Andrade Silva, and O. M. Bruno, "A rotation invariant face recognition method based on complex network," in *Progress in Pattern Recognition, Image Analysis, Computer Vision, and Applications*, Lecture Notes in Computer Science (Springer, Berlin, 2010), Vol. 6419.
- ¹⁸A. R. Backes, D. Casanova, and O. M. Bruno, "Texture analysis and classification: A complex network-based approach," *Inf. Sci.* **219**, 168–180 (2013).
- ¹⁹S. Q. Bao, H. B. Xu, H. Wang, and J. Liu, "Influence of boundary extraction operators on boundary shape classification algorithms based on complex networks," in *Proceedings of China Automation Congress 2020, 26 November, Shanghai, China* (IEEE, 2020), ID. 225, pp. 1–6.
- ²⁰L. Nanni, A. Lumini, and S. Brahnam, "Survey on LBP based texture descriptors for image classification," *Expert Syst. Appl.* **39**(3), 3634–3641 (2012).
- ²¹J. S. Weszka, C. R. Dyer, and A. Rosenfeld, "A comparative study of texture measures for terrain classification," *IEEE Trans. Syst. Man Cybern. SMC-6*(4), 269–285 (1976).
- ²²G. Wang, "Rotation-invariant texture classification based on angular radial transform," *Comput. Mod.* **13**(6), 46–50 (2015).
- ²³Z. J. Fang, Y. G. Fu, and J. H. Chen, "Belief rule base inference for texture image classification," *J. Appl. Sci. Electron. Inf. Eng.* **35**(5), 545–558 (2017).
- ²⁴Q. Ni, J. Kang, M. Tang, Y. Liu, and Y. Zou, "Learning epidemic threshold in complex networks by convolutional neural network," *Chaos* **29**(11), 113106 (2019).
- ²⁵S. Leng, Z. Xu, and H. Ma, "Reconstructing directional causal networks with random forest: Causality meeting machine learning," *Chaos* **29**(9), 093130 (2019).
- ²⁶A. E. Hramov, V. Maksimenko, A. Koronovskii, A. E. Runnova, M. Zhuravlev, A. N. Pisarchik, and J. Kurths, "Percept-related EEG classification using machine learning approach and features of functional brain connectivity," *Chaos* **29**(9), 093110 (2019).

- ²⁷J. Iacobacci and L. Lacasa, “Visibility graphs for image processing,” *IEEE Trans. Pattern Anal. Mach. Intell.* **42**(4), 974–987 (2019).
- ²⁸R. Criado, M. Romance, and A. Sanchez, “A post-processing method for interest point location in images by using weighted line-graph complex networks,” *Int. J. Bifurcat. Chaos* **22**(07), 1250163 (2012).
- ²⁹S. Hossain and S. Serikawa, “Texture databases—A comprehensive survey,” *Pattern Recogn. Lett.* **34**(15), 2007–2022 (2013).
- ³⁰A. Safia and D. C. He, “New Brodatz-based image databases for gray-scale color and multiband texture analysis,” *ISRN Mach. Vision* **2013**, 1–14.